Materials Science-Poland, Vol. 23, No. 3, 2005

Synthesis and structural characterization of a series of transition metal complexes with a tetradentate Schiff-base ligand derived from salicylaldehyde and 2-(2-aminoethylamino)ethanol*

M. MIKURIYA**, K. MATSUNAMI

Department of Chemistry and Open Research Center for Coordination Molecule-based Devices, School of Science and Technology, Kwansei Gakuin University, 2-1 Gakuen, Sanda 669-1337, Japan

A series of transition metal complexes with 1-[(2-hydroxyethyl)amino]-2-(salicylideneamino)ethane (H_2hase), [V(Hhase)$_2$]Cl (**1**), [VO_2(Hhase)] (**2**), [Cr(Hhase)$_2$]Cl (**3**), [Mn(Hhase)$_2$]Cl (**4**), [Fe(Hhase)$_2$]Cl (**5**), [Co(Hhase)$_2$]Cl (**6**), [Co(Hhase)$_2$]Br (**7**), [Co(Hhase)$_2$]I (**8**), [Co(Hhase)$_2$]NO_3 (**9**), [Co(Hhase)$_2$]NCS (**10**), [Co(Hhase)$_2$]ClO_4 (**11**), and [Co(Hhase)$_2$]$CH_3CO_2 \cdot H_2O$ (**12**), have been synthesized by template reactions of salicylaldehyde and 2-(2-aminoethylamino)ethanol with metal salts and characterized by infrared and electronic spectra and magnetic moments. The molecular structures of these complexes were determined by single-crystal X-ray structure analysis. All complexes, except for **2**, are mononuclear with an octahedral metal(III) ion, and the two Hhase ligands act as a meridional tridentate chelate forming hydrogen bonds with the counter anion. The two Hhase ligands are arranged so that the imino-nitrogen atoms are *trans,* while the phenoxo-oxygen atoms and the amino-nitrogen atoms are *cis*. Complex **2** comprises two vanadium (V) atoms with dioxo-bridges. A similar template reaction with copper(II) afforded [Cu(salen)] (H_2salen = *N*,*N*′-bis (salicylidene)ethylendiamine) (**13**) in a low yield.

Key words: *Schiff-base; first transition metal complex*

1. Introduction

There has been a considerable interest in the coordination chemistry of Schiff-base ligands, because of their feasibleness to make various kinds of metal complexes [1, 2]. This has resulted in a vast number of reports on Schiff-base metal complexes. Especially, salen-type tetradentate ligands (H_2salen = *N*,*N*′-bis(salicylidene)ethylendiamine) have been known since 1933 [3], their complexes became a standard system in

---

*The paper presented at the 14th Winter School on Coordination Chemistry, Karpacz, Poland, 6–10 December, 2004.

**Corresponding author, e-mail: junpei@ksc.kwansei.ac.jp

coordination chemistry, and their application as inorganic-organic composite materials was examined. We have been engaged in the chemistry of metal Schiff-base compounds with bridging groups [4–14]. Among Schiff-base-ligands, 1-[(2-hydroxyethyl)amino]-2-(salicylideneamino)ethane (H_2hase) is a unique ligand, which has a phenolic atom and alcoholic oxygen atom as potential bridging groups [9].

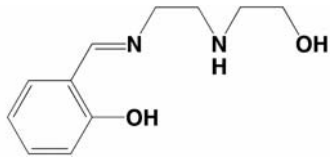

H_2hase

Although complexes of Schiff-base ligands have been reported for a number of transition metals, only a few crystal structures of metal complexes with 1-[(2-hydroxyethyl)amino]-2-(salicylideneamino)ethane have been reported. In the case of the manganese(III) complex, [Mn(Hhase)$_2$]Br, the two Hhase ligands coordinate to the metal atom meridionally, forming intramolecular hydrogen bonds with the counter anion [9]. This intramolecular hydrogen bonding could be interesting for potential inorganic-organic composite materials, because it may contribute to the stability of the metal complex and some functionalities such as anion-binding. Nonetheless, there are still few examples of metal complexes having intramolecular hydrogen bonds. In order to obtain more information on the coordination chemistry of this ligand, we have undertaken a systematic effort to prepare and structurally characterize the complexes formed by the Schiff-base ligand and first row transition metals, because the intra-hydrogen-bonding system is the case for the manganese(III) ion and no other such metal complexes are known to form for other metal ions. Herein we report our findings on vanadium(III), chromium(III), manganese(III), iron(III), and cobalt(III) complexes with the Schiff-base ligand H_2hase.

2. Experimental

Syntheses of the complexes. All reagents and solvents were purchased from commercial sources and used as received. All syntheses were performed under aerobic condition, except where specifically mentioned.

[V(Hhase)$_2$]Cl (1). The manipulation for the preparation of this compound was carried out under Ar using standard Schlenk techniques. To an ethanol (10 ml) solution containing 2-(2-aminoethylamino)ethanol (120 mg, 1.2 mmol) and salicylaldehyde (103 mg, 0.84 mmol), vanadium(III) chloride (32 mg, 0.20 mmol) was added while stirring. The solution was placed at room temperature for three days. Purple plates were deposited and collected by filtration and dried *in vacuo* over P_2O_5: Yield 33 mg (33% on the basis of vanadium(III) chloride used). Found: C, 52.58; H, 5.99;

N, 11.35%. Calcd. for $C_{22}H_{30}ClN_4O_4V$: C, 52.75; H, 6.04; N, 11.19%. IR(hexachloro-1,3 -butadiene, cm^{-1}): ν(OH) 3460 (sh), 3336; ν(NH) 3130, 3058; ν(C=N) 1613. μ_{eff}(288 K), μ_B 2.71. Λ_M (MeOH), $S \cdot mol^{-1} \cdot cm^2$ 120 (lit, range for 1:1 electrolytes [15], 80–115 $S \cdot mol^{-1} \cdot cm^2$). Diffuse reflectance spectrum: λ_{max}, nm 357, 525 sh. Electronic spectrum in MeOH λ_{max}, nm (ε, $dm^3 \cdot mol^{-1} \cdot cm^{-1}$) 312 (6030), 357 (7170), 395 sh (4660).

[VO_2(Hhase)] (2). To an ethanol (10 ml) solution of 2-(2-aminoethylamino)ethanol (128 mg, 1.2 mmol) and salicylaldehyde (103 mg, 0.64 mmol), vanadium(IV) oxydichloride (32 mg, 0.24 mmol) was added while stirring. The mixture was then filtered to remove any material that did not dissolve. After the filtrate was allowed to stand for one day at room temperature in air, pale yellow crystals appeared, which were filtered and dried in vacuo over P_2O_5: yield, 26 mg (42% on the basis of vanadium(IV) oxydichloride used). Found: C, 45.63; H, 5.18; N, 9.75%. Calcd. for $C_{11}H_{15}N_2O_4V$: C, 45.53; H, 5.21; N, 9.65%. IR(hexachloro-1,3-butadiene, cm^{-1}) ν(OH) 3334 (br); ν(NH) 3200 (s); ν(C=N) 1643 (s)). μ_{eff} (288 K), μ_B diamagnetic. Λ_M (MeOH), $S \cdot mol^{-1} \cdot cm^2$ 20. Diffuse reflectance spectrum: λ_{max}, nm 261, 351. Electronic spectrum in MeOH λ_{max}, nm (ε, $dm^3 \cdot mol^{-1} \cdot cm^{-1}$) 253 (10 700), 315 (3680), 480sh (800).

[$Cr(Hhase)_2$]Cl (3). 2-(2-Aminoethylamino)ethanol (122 mg, 1.2 mmol) and salicylaldehyde (103 mg, 0.84 mmol) were dissolved in ethanol (10 ml), then chromium(III) chloride hexahydrate (28 mg, 0.11 mmol) was added while stirring. After the mixture was allowed to stand for ten days at room temperature, dark-brown crystals appeared, which were filtered and dried *in vacuo* over P_2O_5: yield, 28 mg (51% on the basis of chromium(III) chloride hexahydrate used). Found: C, 52.32; H, 6.08; N, 10.91%. Calcd. for $C_{22}H_{30}ClCrN_4O_4$: C, 52.64; H, 6.02; N, 11.16%. IR(hexachloro-1,3-butadiene, cm^{-1}) ν(OH) 3420 (sh), 3336 (br); ν(NH) 3130 (s), 3058 (s); ν(C=N) 1613 (s). μ_{eff} (288 K), μ_B 3.65. Λ_M (MeOH), $S \cdot mol^{-1} \cdot cm^2$ 75. Diffuse reflectance spectrum: λ_{max}, nm 266, 417, 500 (sh), 625 (sh). Electronic spectrum in MeOH λ_{max}, nm (ε, $dm^3 \cdot mol^{-1} \cdot cm^{-1}$) 273 (18800), 397 (3570), 500sh (229).

[$Mn(Hhase)_2$]Cl (4). 2-(2-Aminoethylamino)ethanol (122 mg, 1.2 mmol) and salicylaldehyde (103 mg, 0.84 mmol) were dissolved in ethanol (10 ml), then manganese(II) chloride tetrahydrate (43 mg, 0.22 mmol) was added while stirring. The solution was allowed to stand for three days to give dark brown crystals, which were collected by filtration and dried *in vacuo* over P_2O_5: yield, 56 mg (51% on the basis of manganese(II) chloride tetrahydrate used). Found: C, 52.34; H, 6.21; N, 11.10%. Calcd. for $C_{22}H_{30}ClMnN_4O_4$: C, 52.36; H, 5.99; N, 11.24%. IR(hexachloro -1,3-butadiene, cm^{-1}) ν(OH) 3420 (sh), 3356 (br); ν(NH) 3176 (s), 3032 (s); ν(C=N) 1616 (s). μ_{eff} (288 K), μ_B 5.12. Λ_M (MeOH), $S \cdot mol^{-1} \cdot cm^2$ 83. Diffuse reflectance spectrum: λ_{max}, nm 277, 403, 525sh, 1350. Electronic spectrum in MeOH λ_{max}, nm (ε, $dm^3 \cdot mol^{-1} \cdot cm^{-1}$) 241 (21900), 300 (9780), 390 (2910), 580 (234).

[$Fe(Hhase)_2$]Cl (5). 2-(2-Aminoethylamino)ethanol (122 mg, 1.2 mmol) and salicylaldehyde (103 mg, 0.84 mmol) were dissolved in ethanol (10 ml), then iron(III)

chloride hexahydrate (33 mg, 0.12 mmol) was added while stirring. The solution was allowed to stand for three days to give dark brown crystals, which were collected by filtration and dried *in vacu*o over P_2O_5: yield, 45 mg (73% on the basis of iron(III) chloride hexahydrate used). Found: C, 52.18; H, 5.99, N, 11.38%. Calcd. for $C_{22}H_{30}FeN_4O_4Cl$: C, 52.24; H, 5.98; N, 11.08%. IR(hexachloro-1,3-butadiene, cm^{-1}) ν(OH) 3440 (sh), 3340 (br); ν(NH) 3114 (s), 3058 (s); ν(C=N) 1622 (s). μ_{eff} (288 K), μ_B 5.68. Λ_M (MeOH), $S \cdot mol^{-1} \cdot cm^2$, 86. Diffuse reflectance spectrum: λ_{max}, nm 325, 537, 634. Electronic spectrum in MeOH λ_{max}, nm (ε, $dm^3 \cdot mol^{-1} \cdot cm^{-1}$) 260 (26100), 321 (8740), 501 (1840).

[Co(Hhase)$_2$]Cl (6). 2-(2-Aminoethylamino)ethanol (158 mg, 1.5 mmol) and salicylaldehyde (124 mg, 1.0 mmol) were dissolved in ethanol (10 ml), then cobalt(II) chloride hexahydrate (37 mg, 0.16 mmol) was added while stirring. The solution was left to stand for three days at room temperature to give dark brown crystals, which were collected by filtration and dried in vacuo over P_2O_5: yield, 41 mg (50% on the basis of cobalt(II) chloride hexahydrate used). Found: C, 52.14; H, 6.02; N, 11.06%. Calcd. for $C_{22}H_{30}ClCoN_4O_4$: C, 51.93; H, 5.94; N, 11.01%. IR(hexachloro-1,3 -butadiene, cm^{-1}) ν(OH) 3440 (sh), 3338 (br); ν(NH) 3112 (s), 3042 (s); ν(C=N) 1640 (s).μ_{eff} (288 K), μ_B diamagnetic. Λ_M (MeOH), $S \cdot mol^{-1} \cdot cm^2$ 79. Diffuse reflectance spectrum: λ_{max}, nm 306, 394, 484, 641, 1200. Electronic spectrum in MeOH λ_{max}, nm (ε, $dm^3 \cdot mol^{-1} \cdot cm^{-1}$) 246 (52800), 300 (8810), 385 (5380), 475 (881), 640 (95).

[Co(Hhase)$_2$]Br (7). The complex was prepared in the same way as Co(Hhase)$_2$]Cl, except that cobalt(II) bromide hexahydrate was used instead of cobalt(II) chloride hexahydrate: yield, 46 mg (69% on the basis of cobalt(II) bromide hexahydrate used). Found: C, 47.97; H, 5.49; N, 10.13%. Calcd. for $C_{22}H_{30}BrCoN_4O_4$: C, 47.75; H, 5.46; N, 10.13%. IR(hexachloro-1,3-butadiene, cm^{-1}) ν(OH) 3460 (sh), 3358 (br); ν(NH) 3114 (s), 3058 (s); ν(C=N) 1640 (s). μ_{eff} (288 K), μ_B diamagnetic. Λ_M (MeOH), $S \cdot mol^{-1} \cdot cm^2$ 88. Diffuse reflectance spectrum: λ_{max}, nm 307, 400, 490, 646. Electronic spectrum in MeOH λ_{max}, nm (ε, $dm^3 \cdot mol^{-1} \cdot cm^{-1}$) 246 (40700), 300 (7890), 385 (4360), 475 (868), 639 (87).

[Co(Hhase)$_2$]I (8). The complex was prepared in the same way as [Co(Hhase)$_2$]Cl, except that cobalt(II) iodide hexahydrate was used instead of cobalt(II) chloride hexahydrate: yield, 44 mg (67% on the basis of cobalt(II) iodide hexahydrate used). Found: C, 44.02; H, 5.04; N, 9.33%. Calcd. for $C_{22}H_{30}CoIN_4O_4$: C, 44.26; H, 5.10; N, 9.30%. IR(hexachloro-1,3-butadiene, cm^{-1}) ν(OH) 3390 (br); ν(NH) 3104 (s); ν(C=N) 1636 (s). μ_{eff} (288 K), μ_B diamagnetic. Λ_M (MeOH), $S \cdot mol^{-1} \cdot cm^2$ 94. Diffuse reflectance spectrum: λ_{max}, nm 303, 396, 481, 642. Electronic spectrum in MeOH λ_{max}, nm (ε, $dm^3 \cdot mol^{-1} \cdot cm^{-1}$) 235 (41700), 305 (7350), 385 (4570), 470 (833), 641 (100).

[Co(Hhase)$_2$]NO$_3$ (9). The complex was prepared in the same way as [Co(Hhase)$_2$]Cl, except that cobalt(II) nitrate hexahydrate was used instead of cobalt(II) chloride hexahy-

drate: yield, 17 mg (24% on the basis of cobalt(II) nitrate hexahydrate used). Found: C, 49.44; H, 5.83; N, 13.22%. Calcd. for $C_{22}H_{30}CoN_5O_7$: C, 49.35; H, 5.65; N, 13.08%. IR(hexachloro-1,3-butadiene, cm^{-1}) ν(OH) 3396 (br); ν(NH) 3190 (s), 3046 (s); ν(C=N) 1639 (s). μ_{eff} (288 K), μ_B diamagnetic. Λ_M (MeOH), $S \cdot mol^{-1} \cdot cm^2$ 96. Diffuse reflectance spectrum: λ_{max}, nm 304, 397, 482, 645. Electronic spectrum in MeOH λ_{max}, nm (ε, $dm^3 \cdot mol^{-1} \cdot cm^{-1}$) 246 (49200), 300 (8890), 385 (4860), 475 (961), 642 (99).

[Co(Hhase)$_2$]NCS (10). The complex was prepared in the same way as [Co(Hhase)$_2$]Cl, except that cobalt(II) thiocyanate was used instead of cobalt(II) chloride hexahydrate: yield, 76 mg (65% on the basis of cobalt(II) thiocyanate used). Found: C, 51.69; H, 5.64; N, 13.30%. Calcd. for $C_{23}H_{30}CoN_5O_4S$: C, 51.97; H, 5.69; N, 13.18%. IR(hexachloro-1,3-butadiene, cm^{-1}) ν(OH) 3352 (br); ν(NH) 3212 (s), 3158 (s); ν(C=N) 1643 (s). μ_{eff} (288 K), μ_B diamagnetic. Λ_M (MeOH), $S \cdot mol^{-1} \cdot cm^2$ 90. Diffuse reflectance spectrum: λ_{max}, nm 305, 392, 478, 645. Electronic spectrum in MeOH λ_{max}, nm (ε, $dm^3 \cdot mol^{-1} \cdot cm^{-1}$) 246 (40100), 300 (7140), 385 (4370), 475 (761), 642 (90).

[Co(Hhase)$_2$]ClO$_4$ (11). The complex was prepared in the same way as [Co(Hhase)$_2$]Cl, except that cobalt(II) perchlorate hexahydrate was used instead of cobalt(II) chloride hexahydrate: yield, 35 mg (51% on the basis of cobalt(II) perchlorate hexahydrate used). Found: C, 46.10; H, 5.66; N, 9.80%. Calcd. for $C_{22}H_{30}ClCoN_4O_{12}$: C, 46.12; H, 5.28; N, 9.78%. IR(hexachloro-1,3-butadiene, cm^{-1}) ν(OH) 3510 (br); ν(NH) 3234 (s); ν(C=N) 1633 (s). μ_{eff} (288 K), μ_B diamagnetic. Λ_M (MeOH), $S \cdot mol^{-1} \cdot cm^2$ 119. Diffuse reflectance spectrum: λ_{max}, nm 304, 396, 479, 639. Electronic spectrum in MeOH λ_{max}, nm (ε, $dm^3 \cdot mol^{-1} \cdot cm^{-1}$) 251 (38900), 305 (4700), 386 (3810), 480 (473), 645 (85).

[Co(Hhase)$_2$]CH$_3$CO$_2$·H$_2$O (12). The complex was prepared in the same way as [Co(Hhase)$_2$]Cl, except that cobalt(II) acetate tetrahydrate was used instead of cobalt(II) chloride hexahydrate: yield, 28 mg (34% on the basis of cobalt(II) acetate tetrahydrate used). Found: C, 52.36; H, 6.41; N, 10.18%. Calcd. for $C_{24}H_{35}CoN_5O_7$: C, 52.25; H, 6.26; N, 10.45%. μ_{eff} (288 K), μ_B diamagnetic. Λ_M (MeOH), $S \cdot mol^{-1} \cdot cm^2$ 67. Diffuse reflectance spectrum: λ_{max}, nm 307, 389, 475, 627. Electronic spectrum in MeOH λ_{max}, nm (ε, $dm^3 \cdot mol^{-1} \cdot cm^{-1}$) 246 (44000), 305 (7860), 384 (4500), 470 (879), 639 (93).

[Cu(salen)] (13). 2-(2-Aminoethylamino)ethanol (100 mg, 0.96 mmol) and salicylaldehyde (90 mg, 0.74 mmol) were dissolved in ethanol (5 ml), then copper(II) chloride dihydrate (32 mg, 0.19 mmol) was added while stirring. After adding 50 mg (0.85 mmol) of triethylamine, the resulting solution was allowed to stand for two weeks to give dark violet crystals, which were collected by filtration and dried *in vacuo* over P_2O_5: yield, 8 mg (13% on the basis of copper(II) chloride dihydrate used). IR(hexachloro-1,3-butadiene, cm^{-1}) ν(C=N) 1646, 1628.

Measurements. Carbon, hydrogen, and nitrogen analyses were carried out using a Perkin-Elmer 2400 Series II CHNS/O Analyzer. Infrared spectra were recorded with a JASCO Infrared Spectrometer model IR700 in the 4000–400 cm^{-1} region on a hexachloro-1,3-butadiene mull. Electronic conductivities were measured on a Horiba conductivity meter DS-14. Electronic spectra were measured with a Shimadzu UV-vis –NIR Recording Spectrophotometer Model UV-3100. Room-temperature magnetic moments were determined with a Sherwood MSB-AUTO magnetic susceptibility balance. Susceptibilities were corrected for the diamagnetism of the constituent atoms using Pascal's constants [16]. The effective magnetic moments were calculated from the equation $\mu_{\text{eff}} = 2.828\sqrt{\chi_{\text{M}}T}$, where χ_{M} is the molar magnetic susceptibility.

X-Ray crystal structure analysis. Unit-cell parameters and intensities were measured on an Enraf–Nonius CAD4 diffractometer using graphite-monochromated Mo-K_α radiation at 25±1 °C. Unit-cell parameters were determined by least-squares refinement based on 25 reflections with $20° \le 2\theta \le 30°$.

Table 1. Crystal data of the complexes

Complex	[V(Hhase)$_2$]Cl (**1**)	[VO_2(Hhase)] (**2**)	[Cr(Hhase)$_2$]Cl (**3**)
Formula	$C_{22}H_{30}VN_4O_4Cl$	$C_{11}H_{15}VN_2O_4$	$C_{22}H_{30}CrN_4O_4Cl$
F.W.	500.90	290.19	501.95
Crystal system	monoclinic	monoclinic	monoclinic
Space group	$P2_1/n$	$P2_1/n$	$P2_1/n$
a, Å	9.885(6)	11.239(5)	9.918(6)
b, Å	24.97(1)	6.830(2)	24.81(1)
c, Å	10.514(6)	16.052(8)	10.445(7)
β, °	115.63(3)	105.20(2)	116.08(3)
V, Å^3	2339(2)	1189(1)	2309(2)
Z	4	4	4
D_m, g·cm^{-3}	1.40	1.43	1.44
D_c, g·cm^{-3}	1.42	1.44	1.44
μMo-K_α, cm^{-1}	5.59	8.062	6.336
Crystal size, mm	0.35×0.30×0.20	0.43×0.23×0.20	0.40×0.35×0.15
F(000)	1048	600	1052
2θ range, °	1.0–48.0	1.0–50.0	1.0–48.0
Total No. of observed reflections	3765	2305	3731
No. of observations ($I \ge 3\sigma$)	1384	1111	1752
Total No. of variables	289	163	289
h;k;l range	–11/11; 0/28; 0/12	–13/13; 0/8; 0/19	–11/11; 0/28; 0/12
Largest diff. peak, eÅ^{-3}	0.299	0.615	0.291
R	0.047	0.059	0.048
R_w	0.052	0.068	0.055

Table 1 (continued)

Complex	[Mn(Hhase)$_2$]Cl (**4**)	[Fe(Hhase)$_2$]Cl (**5**)
Formula	$C_{22}H_{30}MnN_4O_4Cl$	$C_{22}H_{30}FeN_4O_4Cl$
F.W.	504.90	505.80
Crystal system	monoclinic	monoclinic
Space group	$P2_1/n$	$P2_1/n$
a, Å	9.880(3)	9.857(3)
b, Å	25.299(3)	24.936(3)
c, Å	10.437(3)	10.470(3)
β, °	116.59(1)	115.71(1)
V, Å^3	2232.9(9)	2318(1)
Z	4	4
D_m, g·cm^{-3}	1.43	1.46
D_c, g·cm^{-3}	1.44	1.45
μMo-K$_\alpha$, cm^{-1}	6.931	7.999
Crystal size, mm	0.30×0.24×0.21	0.40×0.25×0.17
F(000)	1056	1060
2θ range, °	1.0–48.0	1.0–46.0
Total No. of observed reflections	3757	3315
No. of observations ($I \geq 3\sigma$)	2412	2420
Total No. of variables	289	289
h;k;l range	–11/11; 0/29; 0/11	–10/10; 0/29; 0/11
Largest diff. peak, eÅ^{-3}	0.488	0.273
R	0.037	0.031
R_w	0.040	0.033

Complex	[Co(Hhase)$_2$]Cl (**6**)	[Co(Hhase)$_2$]Br (**7**)	[Co(Hhase)$_2$]I (**8**)
Formula	$C_{22}H_{30}CoN_4O_4Cl$	$C_{22}H_{30}CoN_4O_4Br$	$C_{22}H_{30}CoN_4O_4I$
1	2	3	4
F.W.	508.89	553.34	600.34
Crystal system	monoclinic	monoclinic	monoclinic
Space group	$P2_1/n$	$P2_1/n$	$P2_1/n$
a, Å	9.828(3)	9.806(2)	9.788(2)
b, Å	24.913(3)	25.070(3)	24.344(3)
c, Å	10.427(3)	10.486(3)	11.080(3)
β, °	115.89(1)	115.041(9)	111.11(1)
V , Å^3	2297(1)	2335.6(9)	2463(1)
Z	4	4	4
D_m, g·cm^{-3}	1.50	1.63	1.62
D_c, g·cm^{-3}	1.49	1.60	1.62
μMo-K$_\alpha$, cm^{-1}	8.968	24.63	19.67
Crystal size, mm	0.37×0.25×0.19	0.43×0.18×0.17	0.45×0.21×0.19
F(000)	1072	1136	1208
2θ range, °	1.0–47.0	1.0–48.0	1.0–48.0
Total No. of observed reflections	3471	3764	3973

Table 1 (continued)

1	2	3	4
No. of observations ($I \geq 3\sigma$)	2420	2258	2812
Total No. of variables	289	289	289
$h;k;l$ range	−11/11; 0/27; 0/11	−11/11; 0/28; 0/11	−11/11; 0/27; 0/12
Largest diff. peak, eÅ^{-3}	0.256	0.353	0.614
R	0.030	0.034	0.039
R_w	0.033	0.037	0.043

Complex	$[Co(Hhase)_2]NO_3$ (**9**)	$[Co(Hhase)_2]NCS$ (**10**)	$[Co(Hhase)_2]ClO_4$ (**11**)
Formula	$C_{22}H_{30}CoN_5O_8$	$C_{23}H_{30}CoN_5O_4S$	$C_{22}H_{30}CoN_4O_8Cl$
F.W.	551.44	531.52	572.89
Crystal system	$P2_1/n$	$P2_1/n$	$P2_1/n$
Space group	monoclinic	monoclinic	monoclinic
a, Å	9.757(5)	9.798(4)	9.725(2)
b, Å	25.656(6)	22.402(5)	23.590(3)
c, Å	10.532(5)	11.485(4)	11.665(3)
β, °	114.55(2)	108.11(2)	110.98(1)
V , Å^3	2397(1)	2396(1)	2498(1)
Z	4	4	4
D_m, g·cm^{-3}	1.52	1.46	1.53
D_c, g·cm^{-3}	1.53	1.47	1.52
μMo-K$_\alpha$, cm^{-1}	7.628	8.354	8.136
Crystal size, mm	0.35×0.28×0.24	0.50×0.33×0.27	0.51×0.50×0.25
F(000)	1120	1112	1192
2θ range, °	1.0–48.0	1.0–50.0	1.0–48.0
Total No. of observed reflections	3859	4337	4019
No. of observations ($I \geq 3\sigma$)	2043	2258	2812
Total No. of variables	316	289	289
$h;k;l$ range	−11/11; 0/29; 0/12	−11/11; 0/26; 0/13	−11/11; 0/27; 0/13
Largest diff. peak, eÅ^{-3}	0.357	0.353	0.614
R	0.038	0.034	0.039
R_w	0.040	0.037	0.043

Complex	$[Co(Hhase)_2]CH_3CO_2 \cdot H_2O$ (**12**)	[Cu(salen)] (**13**)
Formula	$C_{24}H_{35}CoN_5O_7$	$C_{16}H_{14}CuN_2O_2$
1	2	3
F.W.	550.50	329.85
Crystal system	monoclinic	monoclinic
Space group	$P2_1/n$	$C2/c$
a, Å	9.658(2)	26.64(1)
b, Å	23.827(4)	6.969(5)
c, Å	11.459(3)	14.699(6)
β, °	104.59(1)	97.49(2)

Table 1 (continued)

1	2	3
V, Å^3	2552(1)	2705(2)
Z	4	8
D_m, g·cm^{-3}	1.45	1.63
D_c, g·cm^{-3}	1.43	1.62
μMo-K$_\alpha$, cm^{-1}	8.436	18.80
Crystal size, mm	0.40×0.40×0.20	0.40×0.35×0.21
F(000)	1156	1248
2θ range, °	1.0–48.0	1.0–49.0
Total No. of observed reflections	4113	2463
No. of observations ($I \geq 3\sigma$)	2403	3188
Total No. of variables	316	190
h;k;l range	–11/11; 0/23; 0/17	–31/31; 0/8; 0/17
Largest diff. peak, eÅ^{-3}	0.357	0.484
R	0.038	0.041
R_w	0.040	0.054

The crystal data and details of data collection are given in Table 1. Intensity data were corrected for Lorentz-polarization effects, but not for absorption. The structures were solved by direct methods and refined by the full-matrix least-squares methods. All non-hydrogen atoms were refined with anisotropic thermal parameters. Hydrogen atoms were inserted at their calculated positions and fixed. The final discrepancy factors, $R = \Sigma||F_0| - |F_c||$, $\Sigma|F_0|$ and $R_w = [w\ (|F_0| - |F_c|)^2 / \Sigma w|F_0|^2]^{1/2}$, are listed in Table 1. The weighting scheme, $w = 1/[\sigma^2(|F_0|) + (0.02|F_0|)^2 + 1.0]$, was employed. All calculations were carried out on a VAX station 4000 90A computer using the MolEN program package [17].

3. Results and discussion

The template reaction of an excess amount of 2-(2-aminoethylamino)ethanol and salicylaldehyde in the presence of an appropriate metal chloride in ethanol yielded octahedral trivalent metal complexes with 1-[(2-hydroxyethyl)amino]-2-(salicylideneamino)ethane, [M(Hhase)$_2$]Cl (M = V (**1**), Cr (**3**), Mn (**4**), and Fe (**5**)). In the case of cobalt, the reaction with cobalt(II) salt gave similar octahedral cations, [Co(Hhase)$_2$]$^+$, of which a variety of salts (**6–12**) were isolated as crystalline solids. When H_2hase was reacted with vanadyl chloride in ethanol, pale yellow plates of [VO_2(Hhase)] (**2**) could be isolated. On the other hand, reaction mixture solutions did not yield any precipitate in the cases of nickel(II) and copper(II) except for [Cu(salen)].

The X-ray crystallography of **1** reveals that the complex consists of a six-coordinate V(III) ion, which has a distorted octahedron with two phenoxo-oxygen atoms,

two imino-nitrogen atoms, and two amino-nitrogen atoms of the two Hhase ligands. An ORTEP drawing of the complex with an atom-labelling scheme is shown in Fig. 1. Selected bond lengths and angles are listed in Table. 2. None of the Schiff-base ligands are fully deprotonated and the Hhase ligand acts a meridional tridentate chelate forming a fused 6-5 chelate ring. The two Hhase ligands are arranged so that the imino-nitrogen atoms are *trans,* while the phenoxo-oxygen atoms and the amino-nitrogen atoms are *cis*. The V–O1 and V–O3 distances are 2.002 (7) and 1.861 (7) Å, respectively. The V–N2 (2.257 (9) Å) and V–N4 (2.110 (8) Å) distances are noticeably longer than the V–N1 (2.066 (6) Å) and V–N3 (2.069 (6) Å) distances. The elongation of *trans* V–N bonds relative to V–O can be ascribed to the *trans* influence of the V-phenoxo bonds. Neither of the alcohol groups of the two Hhase ligands are coordinated to the central metal atom, but positioned *cis* to each other, forming hydrogen bonds with the chloride ion, as suggested by the distances O2···Cl – 3.30 (1), O4···Cl – 3.57 (1), O4′···Cl – 3.452 (8), N2···Cl – 3.135 (8), and N4···Cl – 3.566 (8) Å. The effective magnetic moment of **1** is 2.71μ_B at room temperature. This is close to the spin-only value (2.82μ_B) for a d^2 ion.

Table 2. Selected bond distances (Å) and angles (°) of [M(Hhase)$_2$]Cl

Bond	[V(Hhase)$_2$]Cl (**1**)	[Cr(Hhase)$_2$]Cl (**3**)	[Mn(Hhase)$_2$]Cl (**4**)	[Fe(Hhase)$_2$] Cl (**5**)	[Co(Hhase)$_2$] Cl (**6**)
M–O1	2.002(7)	1.933(7)	1.894(3)	1.895(3)	1.896(3)
M–O3	1.861(7)	1.936(7)	2.040(3)	1.902(3)	1.897(2)
M–N1	2.066(6)	2.026(6)	2.001(3)	2.012(2)	1.901(2)
M–N3	2.069(6)	2.009(6)	2.028(4)	2.000(2)	1.903(2)
M–N2	2.257(9)	2.173(8)	2.103(3)	2.115(3)	2.008(3)
M–N4	2.110(8)	2.150(8)	2.334(4)	2.139(3)	2.027(3)
O1–M–N1	83.0(3)	90.0(3)	90.2(1)	90.5(1)	93.6(1)
O3–M–N3	82.7(3)	90.1(3)	88.1(1)	90.6(1)	93.8(1)
N1–M–N2	84.7(3)	81.8(3)	82.1(1)	81.2(1)	84.8(1)
N3–M–N4	84.8(3)	81.8(3)	79.0(1)	81.4(1)	84.7(1)
O1–M–N2	166.9(3)	171.3(2)	172.2(1)	171.6(1)	177.2(1)
O3–M–N4	165.9(3)	171.8(2)	170.0(1)	171.6(1)	178.3(1)
O1–M–O3	99.9(3)	92.8(3)	94.4(1)	94.1(1)	90.4(1)
N1–M–N3	175.6(3)	175.6(3)	174.4(1)	175.1(1)	177.9(1)
N2–M–N4	87.7(3)	92.0(3)	91.6(1)	91.4(1)	93.7(1)

Contrary to the mononuclear nature of **1**, the X-ray crystal analysis of **2** shows the structure to be a dinuclear V(V) cluster. As shown in Fig. 2, an ORTEP diagram of **2** demonstrates that each V(V) ion is six-coordinate with three oxo groups. The first of these (V–O3) is a typical V=O distance of 1.618(8) Å. The second and third oxo groups are involved in the bridges between V and V′, with distances of 1.673(8) and 2.463(7) Å for the V–O4 and V–O4′ bonds, respectively. The remaining three coordination sites are occupied by the phenoxo-oxygen (V–O1 1.919(7) Å), imino-nitrogen

(V–N1 2.151(8) Å), and amino-nitrogen (V–N2 2.164(8) Å) atoms of the Hhase ligand, with the alcohol group remaining uncoordinated. A similar structure of the dinuclear complex prepared by a different method has been reported previously [18]. The complex is diamagnetic, being consistent with the d^0 configuration of V(V).

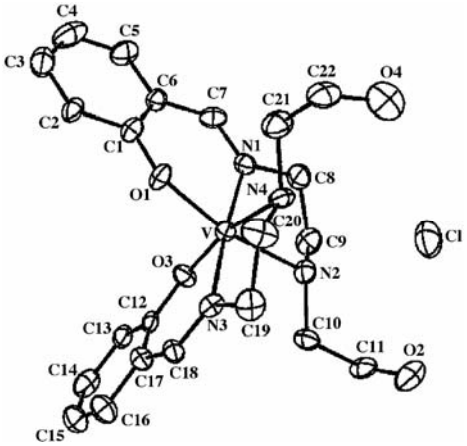

Fig. 1. ORTEP drawing of the structure of $[V(Hhase)_2]Cl$ (**1**), showing the 35% probability thermal ellipsoids and atom labeling scheme

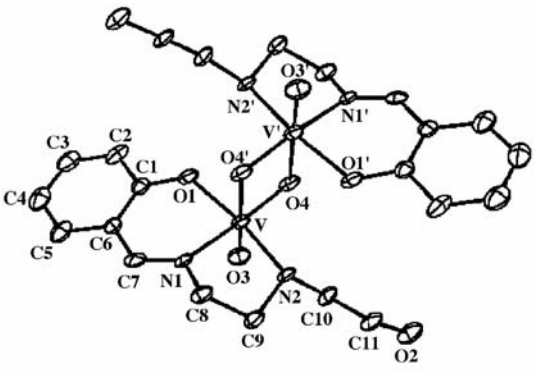

Fig. 2. ORTEP drawing of the structure of $[VO_2(Hhase)]$ (**2**), showing the 35% probability thermal ellipsoids and atom labeling scheme

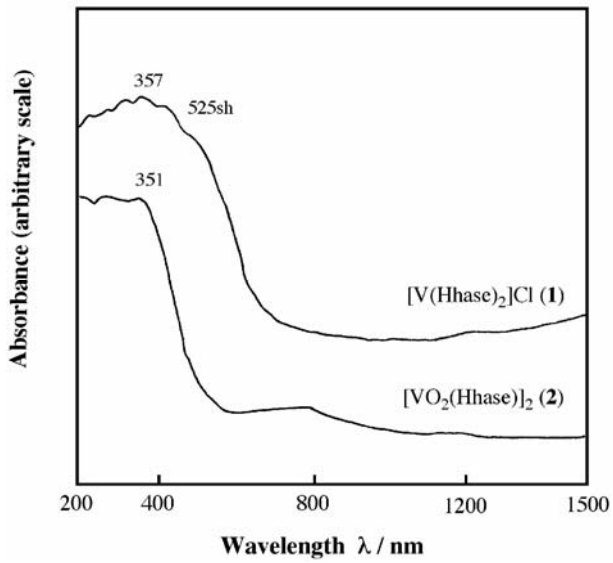

Fig. 3. Diffuse reflectance spectra of $[V(Hhase)_2]$ (**1**) and $[VO_2(Hhase)]$ (**2**)

The diffuse reflectance spectrum of **2** is shown in Fig. 3 together with that of **1**. In the UV region, the high-intensity band observed around 350 nm in both complexes may be due to a ligand-to-metal charge transfer (LMCT) transition, while the other

bands, at still higher energies, can be due to ligand-internal transitions. Contrary to the spectra of **2**, which lacks d-d bands due to the d^0 configuration of V(V), the reflectance spectra of **1** show d-d bands around 525 nm. The d-d bands, however, were hidden by a charge transfer band around 357 nm when the spectrum of **1** was measured in methanol.

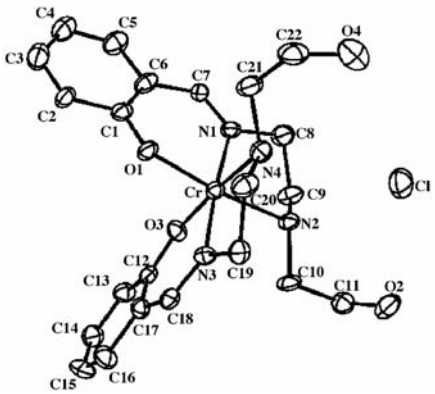

Fig. 4. ORTEP drawing of the structure of $[Cr(Hhase)_2]Cl$ (**3**), showing the 35% probability thermal ellipsoids and atom labeling scheme

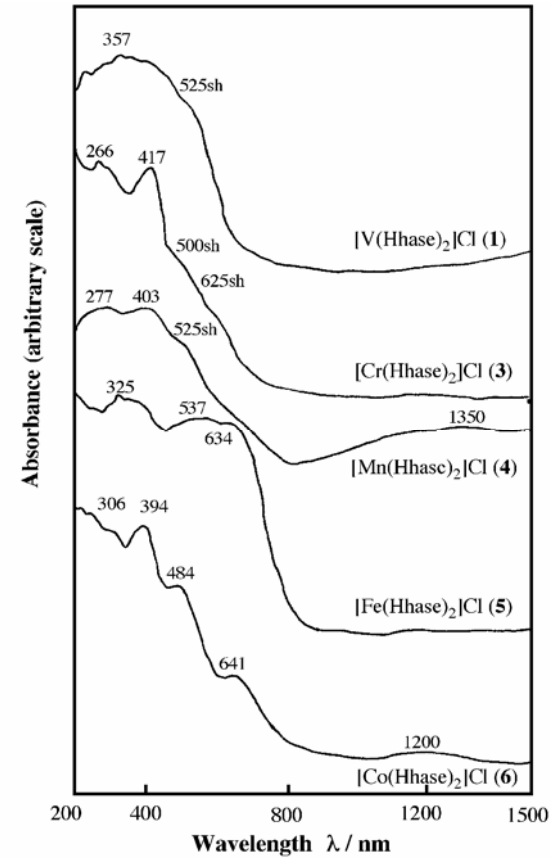

Fig. 5. Diffuse reflectance spectra of $[M(Hhase)_2]Cl$

A perspective view of the crystal structure of **3** is shown in Fig. 4. The molecular structure of the chromium(III) complex is similar to that of the vanadium(III) complex **1**, showing a more octahedral arrangement around the metal ion. The corresponding Cr–O and Cr–N bonds have similar bond lengths: Cr–O1 – 1.933 (7) Å, Cr–O3 – 1.936(7) Å; Cr–N1 – 2.026(6) Å, Cr–N3 – 2.009(6) Å; Cr–N2 – 2.137(8) Å, Cr–N4 – 2.150(8) Å. This structural feature may reflect the d^3 configuration of Cr(III). The magnetic moment of **3** is 3.65μ_B at room temperature, corresponding the spin-only value 3.87μ_B. Both 2-hydroxyethylamino groups of the two Hhase ligands are positioned *cis* with respect to each other, forming hydrogen bonds with the chloride ion, as suggested by the distances O2···Cl – 3.188(9), O4···Cl – 3.54(1), O4′···Cl – 3.322(7), N2···Cl – 3.145(8), and N4···Cl – 3.476(7) Å. The reflectance spectrum of **4** is illustrated in Fig. 5. The shoulder bands around 500 and 625 nm may be assigned to d–d transitions. The intense band at 417 nm and more intense bands around 266 nm may be assigned as a LMCT transition and ligand-internal transitions, respectively.

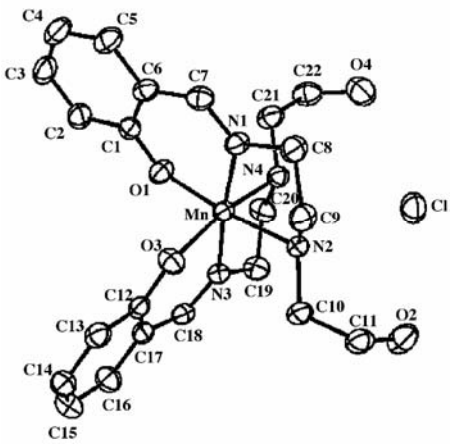

Fig. 6. ORTEP drawing of the structure of $[Mn(Hhase)_2]Cl$ (**4**), showing the 35% probability thermal ellipsoids and atom labeling scheme

The manganese(III) complex **4** is isomorphous with **1** and **3**, and the molecular structure of **4** is similar to those of **1** and **3** (Fig. 6). The most significant difference in **4** is the expected tetragonal Jahn–Teller distortion of the manganese(III) octahedron. The Mn–O1 and Mn–O3 bond distances are 1.894(3) and 2.040(3) Å, respectively, for the phenoxo oxygen. The lengths of the Mn–N bonds range from 2.001(3) for Mn–N1 to 2.334(4) Å for Mn–N4 (Mn–N3 – 2.028(4) Å, Mn–N2 – 2.103(4) Å). These differences in bond lengths are attributed to a Jahn–Teller distortion along the O3-Mn–N4 axis, arising from the d^4 configuration of the manganese centre. This structure is almost the same as that found in $[Mn(Hhase)_2]Br$ [9]. The intramolecular hydrogen bonds O2···Cl, O4···Cl, O4′···Cl, N2···Cl, and N4···Cl have the lengths of 3.175(4), 3.653(5), 3.330(3), 3.190(4), and 3.470(4) Å, respectively. The magnetic moment of **4** is 5.12μ_B at room temperature, which is consistent with a d^4 high-spin system (the spin-only value is 4.90μ_B). The reflectance spectrum of **4** is shown in Fig. 5. The lowest energy band at 1350 nm is assigned to d-d transitions. The shoulder around 525

nm and a stronger band at 403 nm may be assigned to the LMCT transition from p_π orbitals on the phenoxo oxygen to the half-filled Mn(III) d_π^* and d_σ^* orbitals, respectively [19]. The iron(III) complex **5** is isomorphous with **1**, **3**, and **4**, and the molecular structure of **5** is similar to those of **1**, **3**, and **4**. In contrast to **4**, the corresponding Fe–O and Fe–N bonds have similar bond lengths: Fe–O1 – 1.895(3), Fe–O3 – 1.902(3) Å; Fe–N1 – 2.012(2), Fe–N3 – 2.000(2) Å; Fe–N2 – 2.115(3), Fe–N4 – 2.139(3) Å (Fig. 7). This may reflect the high–spin d^5 electronic configuration. There are intramolecular hydrogen bonds between the chloride ion and the alcohol group or amino group of the Hhase ligands, as suggested by the distances O2···Cl – 3.186(4), O4···Cl – 3.493(4), O4′···Cl – 3.391(3), N2···Cl – 3.175(3), and N4···Cl – 3.463(3) Å. In the reflectance spectrum of **5** (Fig. 5), the relatively intense bands around 537 and 325 nm can be assigned to transitions from the p_π orbital on the phenoxo oxygen to the half–filled d_π* and d_σ* orbitals on the iron(III) ion, respectively, whereas d–d transitions should be very weak and difficult to detect for iron(III) due to the high–spin state of the d^5 ion [20]. The magnetic moment of **5** at room temperature(5.68μ_B) is consistent with a d^5 high–spin system (the spin-only value is 5.90μ_B).

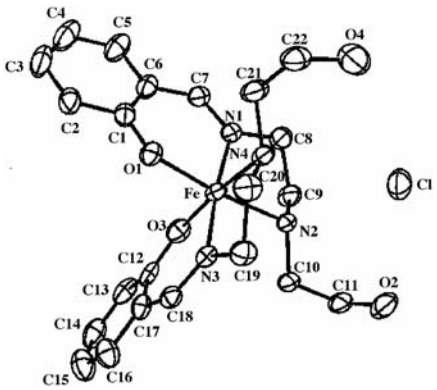

Fig. 7. ORTEP drawing of the structure of [Fe(Hhase)$_2$]Cl (**5**), showing the 35% probability thermal ellipsoids and atom labeling scheme

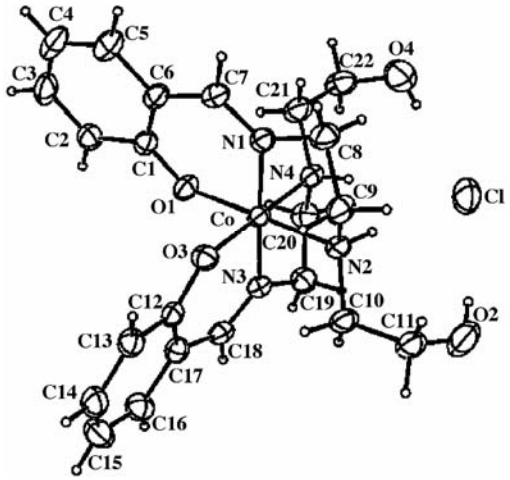

Fig. 8. ORTEP drawing of the structure of [Co(Hhase)$_2$]Cl (**6**), showing the 35% probability thermal ellipsoids and atom labeling scheme

The cobalt(III) complex **6** is also isomorphous with **1**, **3**, **4**, and **5**. As shown in Fig. 8, the molecular structure of **6** is similar to those of **1**, **3**, **4**, and **5**. Among the present [M(Hhase)$_2$]Cl complexes (M = V, Cr, Mn, Fe, Co), the coordination environment around the cobalt(III) ion is closest to a regular octahedral arrangement: Co–O1 – 1.896(3) Å, Co–O3 – 1.897(2) Å; Co–N1 – 1.901(2) Å, Co–N3 – 1.903(2) Å; Co–N2 – 2.008(3) Å, Co–N4 – 2.027(3) Å. This may arise from a large crystal field stabilization energy, which is due to the low–spin d^6 electron configuration of the

Co(III) centre. There are intramolecular hydrogen bonds between the chloride ion and the alcohol group or amino group of the Hhase ligands, as suggested by the distances O2···Cl – 3.174(4), O4···Cl – 3.503(4), O4′···Cl – 3.381(3), N2···Cl – 3.160(3), and N4···Cl – 3.462(3) Å. Complex **6** is diamagnetic as suggested from the low–spin d^6 configuration. The reflectance spectrum of **6** is shown in Fig. 5. The lower energy bands at 641 and 484 nm can be assigned to d–d transitions. The relatively intense band at 394 nm may be assigned to the LMCT transition from the p_π orbital on the phenoxo oxygen to the Co(III) d^*_σ orbitals, while the other bands, at still higher energies, can be due to ligand–internal transitions. Interestingly, the counter anion bound to the $[Co(Hhase)_2]^-$ moiety via hydrogen bonds can be changed to Br^- (**7**), I^- (**8**), NO_3^- (**9**), NCS^- (**10**), ClO_4^- (**11**), or $CH_3CO_2^-$ (**12**) by using a variety of cobalt(II) salts. All of the crystal structures of **6–12** are isomorphous with each other (Figs. 9–14). Selected bond lengths and angles are listed in Table 3.

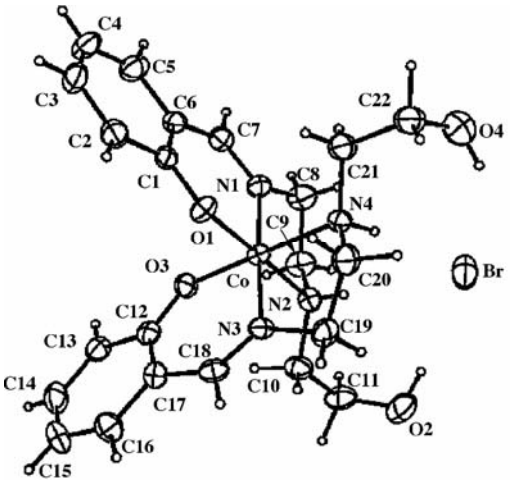

Fig. 9. ORTEP drawing of the structure of $[Co(Hhase)_2]Br$ (**7**), showing the 35% probability thermal ellipsoids and atom labeling scheme

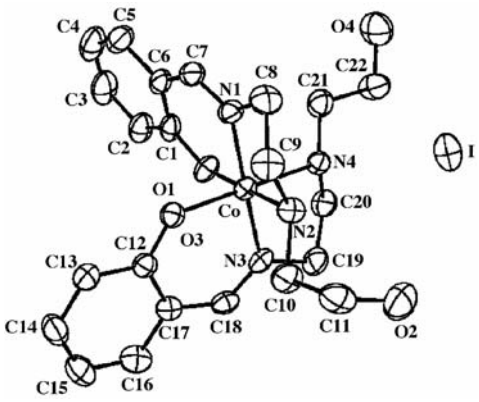

Fig. 10. ORTEP drawing of the structure of $[Co(Hhase)_2]I$ (**8**), showing the 35% probability thermal ellipsoids and atom labeling scheme

Bond lengths and angles around the cobalt ion do not differ significantly from those in **6** and exhibit an octahedral arrangement: Co–O1 – 1.893(4) Å, Co–O3 – 1.898(4) Å, Co–N1 – 1.901(4) Å, Co–N3 – 1.902(4) Å, Co–N2 – 2.002(5) Å, and Co–N4 – 2.030(4) Å for **7**; Co–O1 – 1.879(5) Å, Co–O3 – 1.896(5) Å, Co–N1 – 1.909(5) Å, Co–N3 – 1.902(5) Å, Co–N2 – 2.008(5) Å, and Co–N4 2.011(5) Å for **8**; Co–O1 – 1.892(3) Å, Co–O3 – 1.899(3) Å, Co–N1 – 1.911(3) Å, Co–N3 – 1.910(3) Å, Co–N2 – 2.010(4) Å, and Co–N4 – 2.033(4) Å for **9**; Co–O1 – 1.882(5) Å, Co–O3 – 1.897(5) Å, Co–N1 – 1.900(5) Å, Co–N3 – 1.904(5) Å, Co–N2 – 2.003(6) Å, and Co–N4 2.009(6) Å for **10**; Co–O1 – 1.872(6) Å, Co–O3 – 1.891(5) Å, Co–N1 – 1.899(5) Å, Co–N3 – 1.901(5) Å, Co–N2 – 2.006(7), and Co–N4 – 2.017(7) Å for

11; Co–O1 – 1.896(4) Å, Co–O3 – 1.880(4) Å, Co–N1 – 1.902(4) Å, Co–N3 – 1.893(3) Å, Co–N2 – 2.006(4) Å, andCo–N4 – 1.996(4) Å for **12**.

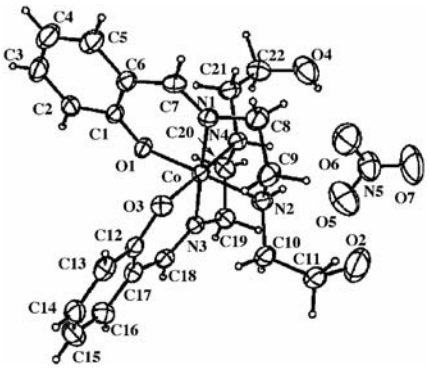

Fig. 11. ORTEP drawing of the structure of $[Co(Hhase)_2]NO_3$ (**9**), showing the 35% probability thermal ellipsoids and atom labeling scheme

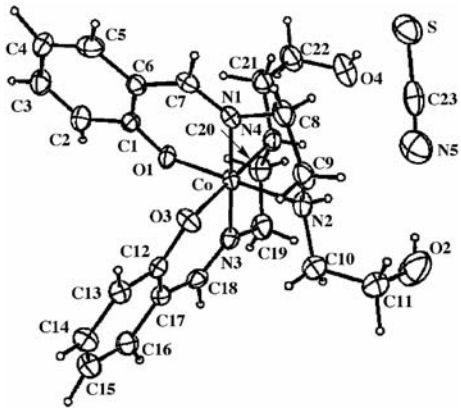

Fig. 12. ORTEP drawing of the structure of $[Co(Hhase)_2]NCS$ (**10**), showing the 35% probability thermal ellipsoids and atom labeling scheme

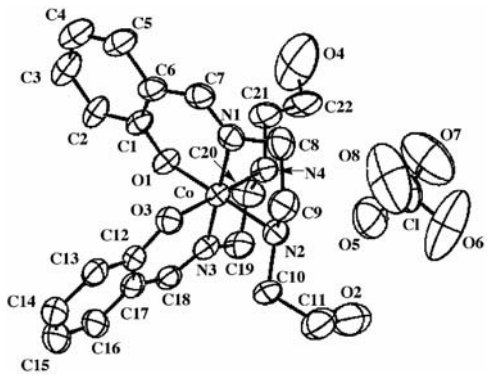

Fig. 13. ORTEP drawing of the structure of $[Co(Hhase)_2]ClO_4$ (**11**), showing the 35% probability thermal ellipsoids and atom labeling scheme

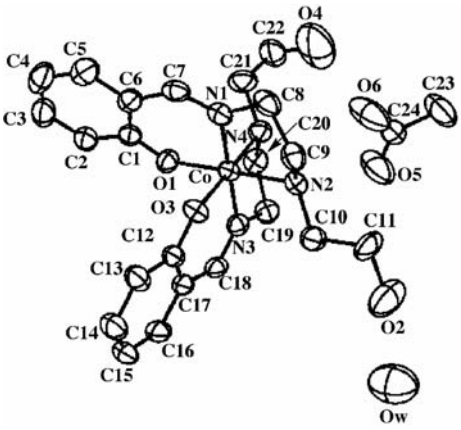

Fig. 14. ORTEP drawing of the structure of $[Co(Hhase)_2]CH_3CO_2 \cdot H_2O$ (**12**), showing the 35% probability thermal ellipsoids and atom labeling scheme

There are intramolecular hydrogen bonds between the counter anion or water molecule (in the case of **12**) and the alcohol group or amino group of the Hhase ligands, and the bond lengths are significantly different depending on the size of the counter anion, as suggested by the distances O2···Br – 3.303(5), O4···Br – 3.573(6), O4′···Br – 3.570(4), N2···Br – 3.342(4), and N4···Br – 3.611(4) Å for **7**; O2···I – 3.457(7), N2···I – 3.565(5), and N4···I – 3.719(5) Å for **8**; O2···O5 – 2.871(8), N2···O6 – 3.009(6), and N4···O6 – 3.285(7) Å for **9**; O2···N5 – 2.85(1), O4···S

Table 3. Selected bond distances (Å) and angles (°) of $[Co(Hhase)_2]X$

Bond	X						
	–Cl (**6**)	–Br (**7**)	–I (**8**)	$–NO_3$ (**9**)	–NCS (**10**)	$–ClO_4$ (**11**)	$–CH_3CO_2·H_2O$ (**12**)
Co–O1	1.896(3)	1.893(4)	1.879(5)	1.892(3)	1.882(5)	1.872(6)	1.896(4)
Co–O3	1.897(2)	1.898(4)	1.896(5)	1.899(3)	1.897(5)	1.891(5)	1.880(4)
Co–N1	1.910(2)	1.901(4)	1.909(5)	1.911(3)	1.900(5)	1.899(5)	1.902(4)
Co–N3	1.903(2)	1.902(4)	1.902(5)	1.910(3)	1.904(5)	1.901(5)	1.893(3)
Co–N2	2.008(3)	2.002(5)	2.008(5)	2.010(4)	2.003(6)	2.006(7)	2.006(4)
Co–N4	2.027(3)	2.030(4)	2.011(5)	2.033(4)	2.009(6)	2.017(7)	1.996(4)
O1–Co–N1	93.6(1)	93.8(2)	93.6(2)	93.5(1)	93.9(2)	94.2(2)	94.7(2)
O3–Co–N3	93.8(1)	93.5(2)	94.5(2)	93.4(1)	94.3(2)	94.5(3)	94.3(2)
N1–Co–N2	84.8(1)	84.9(2)	85.3(2)	85.2(2)	85.3(2)	85.4(3)	85.4(2)
N3–Co–N4	84.7(1)	85.1(2)	84.5(2)	84.9(1)	85.3(2)	84.8(3)	85.6(2)
O1–Co–O3	90.3(1)	90.6(2)	90.9(2)	90.3(1)	91.6(2)	90.7(2)	90.5(2)
N1–Co–N3	177.9(1)	178.2(2)	178.7(2)	178.7(1)	178.4(2)	179.1(3)	178.8(2)
N2–Co–N4	93.7(1)	94.2(2)	92.0(2)	93.6(2)	92.8(2)	92.6(3)	92.8(2)

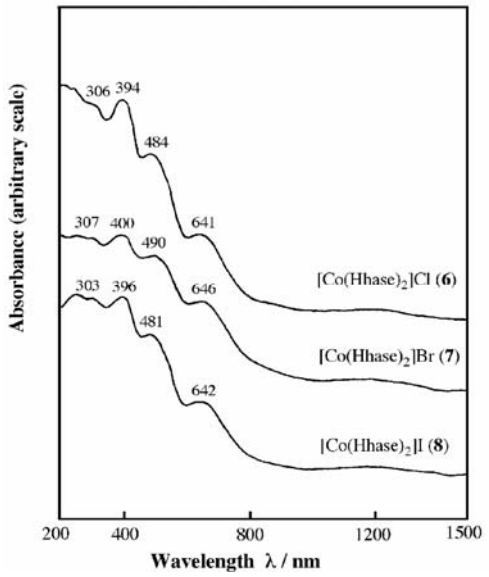

Fig. 15. Diffuse reflectance spectra of $[Co(Hhase)_2]X$ (X = Cl, Br, I)

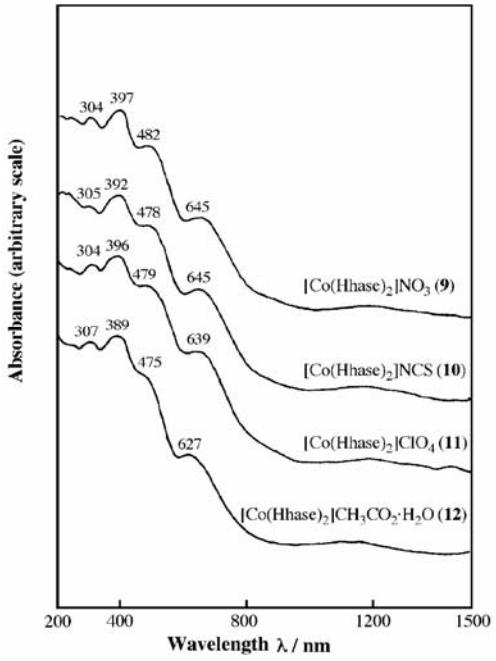

Fig. 16. Diffuse reflectance spectra of $[Co(Hhase)_2]X$ (X = NO_3, NCS, ClO_4, $CH_3CO_2·H_2O$)

– 3.265(6), and N2···N5 – 3.07(1) Å for **10**; O2···O4′ – 2.69(1) Å and O2···O5 – 3.15(2) Å for **11**; O2···OW – 2.79(1), N2···O5 – 2.874(8), and N4···O5 – 3.252(7) Å for **12**. As can be expected from the almost same structures around the metal centres,

the UV–vis spectral features of **7–12** are very similar to that of **6** (Figs. 15 and 16) and all of these cobalt(III) complexes are diamagnetic.

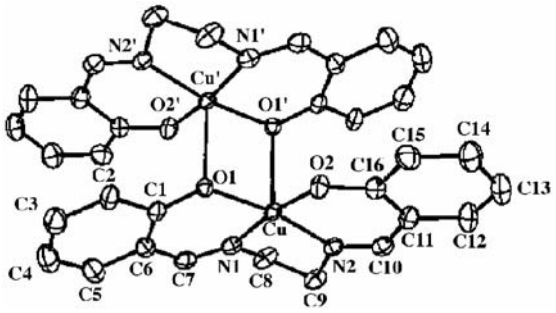

Fig. 17. ORTEP drawing of the structure of [Cu(salen)] (**13**), showing the 35% probability thermal ellipsoids and atom labeling scheme

In the case of the reaction of H_2hase with nickel(II) and copper(II) salts, we could not receive any precipitation materials. This may be due to difficulties in the oxidation of the metal centre for nickel(II) and copper(II) ions, because an oxidation state of three is necessary for the formation of the $[M(Hhase)_2]X$ complexes. We could barely isolate small amounts of crystals of **13** in the reaction with copper(II) chloride dihydrate in ethanol. The X-ray crystal structure analysis of **13**, however, revealed that the complex is a dinuclear copper(II) complex of salen [Cu(salen)], as shown in Fig. 17 – this is a well-known structure of [Cu(salen)] [21]. The formation of the salen ligand suggests that an elimination reaction of the hydroxyethyl group of 2-(2-aminoethylamino)ethanol occurs during the template reaction with salicylaldehyde in the presence of the copper(II) ion [5]. Triethylamine, which was not used in the other cases, may have induced the elimination reaction during the formation of the metal complex.

4. Conclusions

Reactions of excess amounts of the Schiff-base ligand 1-[(2-hydroxyethyl)amino]-2-(salicylideneamino)ethane(H_2hase) with an appropriate metal chloride in ethanol yielded octahedral the trivalent metal complexes $[M(Hhase)_2]Cl$ (M = V (**1**), Cr (**3**), Mn (**4**), Fe (**5**), Co(**6**)). In the case of cobalt compounds, cobalt(III) complexes incorporating different counter anions – $[Co(Hhase)_2]X$ (X = Br (**7**), I (**8**), NO_3 (**9**), NCS (**10**), ClO_4 (**11**), and CH_3CO_2 (**12**)) – can be obtained easily. These counter anions have hydrogen bonds between the *cis*-oriented 2-hydroxyethylamino groups of the two Hhase ligands. The stabilization due to these hydrogen bonds, in addition to the presence (or even the lack) of a crystal field stabilization energy in trivalent metal ions, provided a series of metal complexes with Hhase.

Acknowledgements

The present work was partially supported by the "Open Research Center" Project for Private Universities: matching fund subsidy and Grants-in-Aid for Scientific Research No. 16550062 from the Ministry of Education, Culture, Sports, Science and Technology.

References

[1] CALLIGARIS M., RANDACCIO L., *Comprehensive Coordination Chemistry*, G. Wilkinson, R.D. Gillard, J.A. McCleverty (Eds.), Pergamon Press, Oxford, 1987, Chap. 20.1.

[2] HERNANDEZ-MOLINA R., MEDEROS A., *Comprehensive Coordination Chemistry II*, J.A. McCleverty, T.J. Meyer (Eds.), Elsevier, Oxford, 2004, Chap. 1.19.

[3] PFEIFFER P., BREITH E., LUBBE E., TSUMAKI T., Liebigs Ann. Chem., 503 (1933), 84.

[4] MIKURIYA M., KIDA S., MURASE I., Chem. Lett. 1988, 35; MIKURIYA M., YAMATO Y.TOKII T., Inorg. Chim. Acta, 181 (1991), 1; MIKURIYA M., YAMATO Y., TOKII T., Chem. Lett. (1991), 1429; MIKURIYA M., SASAKI T., ANJIKI A., IKENOUE S., TOKII T., Bull. Chem. Soc. Jpn., 65 (1992), 334; MIKURIYA M., YAMATO Y., TOKII T., Bull. Chem. Soc. Jpn., 65 (1992), 1466; MIKURIYA M., YAMATO Y., TOKII T., Bull. Chem. Soc. Jpn., 65 (1992), 2624; MIKURIYA M., YAMATO Y., TOKII T., Chem. Lett. (1992), 1571.

[5] MIKURIYA M., KAWASAKI Y., TOKII T.T, YANAI S., KAWAMORI A., Inorg. Chim. Acta, 156 (1989), 21; MIKURIYA M., FUJII T., KAMISAWA S., KAWASAKI Y., TOKII T., OSHIO H., Chem. Lett., (1990), 1181; MIKURIYA M., FUJII T., TOKII T., KAWAMORI A., Bull. Chem. Soc. Jpn., 66 (1993), 1675; MIKURIYA M., NAKADERA K., TOKII T., Inorg. Chim. Acta, 194 (1992), 129.

[6] MIKURIYA M., SHIGEMATSU S., KAWANO K., TOKII T., OSHIO H., Chem. Lett. (1990), 729; MIKURIYA M., KAKUTA Y., KAWANO K., TOKII T., Chem. Lett. (1991), 2031; MIKURIYA M., JIE D., KAKUTA Y., TOKII T., Bull. Chem. Soc. Jpn., 66 (1993), 1132; MIKURIYA M., KAKUTA Y., NUKADA R., KOTERA T., TOKII T., Bull. Chem. Soc., Jpn., 74 (2001), 1425.

[7] MIKURIYA M., MAJIMA K., YAMATO Y., Chem. Lett. (1992), 1929; MIKURIYA M., NAGAO N., KONDO K., Chem. Lett. (2000), 516; MIKURIYA M., MINOWA K., Inorg. Chem. Commun., 3 (2000), 227; MIKURIYA M., MINOWA K., LIM J.-W., Bull. Chem. Soc. Jpn., 74 (2001), 331; MIKURIYA M., MINOWA K., NAGAO N., Bull. Chem. Soc. Jpn., 74 (2001), 871; MIKURIYA M., MINOWA K., NAGAO N., Inorg. Chem. Commun., 4 (2001), 441; MIKURIYA M., MINOWA K., NUKADA R., Bull. Chem. Soc., Jpn., 75 (2002), 2595.

[8] MIKURIYA M., NAKADERA K., KOTERA T., Chem. Lett. (1993), 637; MIKURIYA M., NAKADERA K., KOTERA T., TOKII T., MORI W., Bull. Chem. Soc. Jpn., 68 (1995), 3077; MIKURIYA M., NAKADERA K., Chem.Lett. (1995), 213; MIKURIYA M., NAKADERA K., KOTERA T., Bull. Chem. Soc. Jpn., 69, (1996), 399; MIKURIYA M., FUKUYA M., Bull. Chem. Soc. Jpn., 69 (1996), 679; MIKURIYA M., TASHIMA S., Polyhedron, 17 (1998), 207; MIKURIYA M., FUKUYA M., Chem. Lett. (1998), 421; MIKURIYA M., IKEMI S., LIM J.-W., Bull. Chem. Soc. Jpn., 74 (2001) 88; MIKURIYA M., IKEMI S., YAO S., Chem. Lett. (2000), 538; MIKURIYA M., NAKADERA K., LIM J.-W., Synth. React. Inorg. Met.-Org. Chem., 32 (2002), 117.

[9] MIKURIYA M., TAKEBAYASHI H., MATSUNAMI K., Bull. Chem. Soc. Jpn., 67 (1994), 3128.

[10] MIKURIYA M., HASHIMOTO Y., KAWAMORI A., Chem. Lett. (1995), 1095.

[11] MIKURIYA M., YAMAZAKI Y., Chem. Lett. (1995), 373.

[12] MIKURIYA, M., HATANO Y., ASATO E., Chem. Lett. (1996), 849; MIKURIYA M., HATANO Y., ASATO E., Bull. Chem. Soc. Jpn., 70 (1997), 2495; MIKURIYA M., FUKUMOTO H., KAKO T., Inorg. Chem. Commun., 1 (1998), 225.

[13] MIKURIYA M., IKENOUE S., NUKADA R., LIM J.-W., Bull. Chem. Soc., Jpn., 74 (2001), 101.

[14] MIKURIYA M., NUKADA R., TOKAMI W., HASHIMOTO Y., FUJII T., Bull. Chem. Soc. Jpn., 69 (1996), 1573.

[15] GEARY W.J., Coord. Chem. Rev., 7 (1971), 81.
[16] SELWOOD P.W., *Magnetochemistry*, Interscience Publ., New York, 1956, pp. 78, 91.
[17] FAIR C.K., *MolEN Structure Determination System*, Delft Instruments, Delft, 1990.
[18] LI X., LAH M.S., PECORARO V.L., Inorg. Chem. 27 (1988), 4657.
[19] NEVES A., NASCIMENTO O.R., HORNER M., BATISTA A.A., Inorg. Chem. 31 (1992) 4749.
[20] AINSCOUGH E.W., BRODIE M., PLOWMAN J.E., BROWN K.L., ADDISON A.W., GAINSFORD A.R., Inorg. Chem., 19 (1980), 3655.
[21] BAKER E.N., HALL D., MCKINNON A.J., WATERS T.N., Chem. Commun. (1967), 134; BHADBHADE M.M., SRINIVAS D., Inorg. Chem., 32 (1993), 5458.

Received 16 March 2005